

OPERATIONAL EXPERIENCE WITH FAST FIBER-OPTIC BEAM LOSS MONITORS FOR THE ADVANCED PHOTON SOURCE STORAGE RING SUPERCONDUCTING UNDULATORS*

J. Dooling[†], K. Harkay, V. Sajaev, and H. Shang

Advanced Photon Source, Argonne National Laboratory, Argonne, IL, USA

Abstract

Fast fiber-optic (FFO) beam loss monitors (BLMs) installed with the first two superconducting undulators (SCUs) in the Advanced Photon Source storage ring have proven to be a useful diagnostic for measuring deposited charge (energy) during rapid beam loss events. The first set of FFOBLMs were installed outside the cryostat of the short SCU, a 0.33-m long device, above and below the beam centerline. The second set are mounted with the first 1.1-m-long SCU within the cryostat, on the outboard and inboard sides of the vacuum chamber. The next 1.1-m-long SCU is scheduled to replace the short SCU later in 2016 and will be fitted with FFOBLMs in a manner similar to the original 1.1-m device. The FFOBLMs were employed to set timing and voltage for the abort kicker (AK) system. The AK helps to prevent quenching of the SCUs during beam dumps [1] by directing the beam away from the SC magnet windings. The AK is triggered by the Machine Protection System (MPS). In cases when the AK fails to prevent quenching, the FFOBLMs show that losses often begin before detection by the MPS.

INTRODUCTION

High-purity, fused silica fiber optic (FO) cables allow for fast beam loss diagnosis and their use is becoming more widespread [2–4]. They show no transmission loss up to doses of 1 MGy. This rad hardness distinguishes the high-purity fibers from radiation induced attenuation (RIA) fibers; the latter employ transmission loss as a measure of absorbed dose [5, 6]. The FO beam loss monitors (BLMs) provide fast dosimetry [7, 8].

Superconducting undulators (SCUs) have been installed in the insertion device (ID) straight sections of Sectors 1 and 6 (ID01 and ID06) of the Advanced Photon Source (APS) storage ring (SR). SCU0 has been in Sector 6 and SCU1 is in Sector 1; in September 2016, the prototype SCU0 was replaced with a full length 1-m SCU. In [9], we described calibration of the FO BLM for SCU0. The same approach was employed in ID01; however, a constant 4-mm horizontal orbit bump was required in addition to the injection kicker bump.

INSTALLATION

Both CeramOptec and FiberGuide fused-silica fiber bundles are employed; the bundles are composed of individual

200 μm silica core with 220 μm step-index silica-cladded fibers. All bundles are fabricated with a numerical aperture of 0.22. In the case of the FiberGuide cables, bundles of 7 and 61 fibers are used; whereas, the CeramOptec cables are all 61-fiber bundles. The SCU1 fiber bundles are positioned near beam elevation on either side of the vacuum chamber within the cryostat. Both internal SCU1 bundles are composed of 7 fused-silica fibers. A photograph of the upstream end of the inboard portion of the cryostat is presented in Figure 1. The end of the inboard fiber, covered with aluminum foil, is visible on the lower right-hand side (circled in white).



Figure 1: Looking downstream at the inboard FO bundle installed in the SCU1 cryostat (end circled in white).

ANALYSIS

Calibration is done by depositing the charge of a single bunch in the ID straight section where the fibers are located [9]. During multi-bunch fill pattern losses, the charge deposited by each loss pulse is determined from the integrated photomultiplier tube (PMT) output charge over the pulse period calibrated against the single-bunch loss data. For 24-bunch and 324-bunch uniform fill patterns, the loss pulses are clearly resolved. The SR circumference is 1104 m and the rf operates at a harmonic number of 1296 ($f_{rf} = 352$ MHz); thus, in a 24-bunch fill pattern, the loss charge is determined from summing the calibrated charge in each spacing of 54 rf buckets or 154 ns.

Calibration shows the responses of the PMTs to be nonlinear with respect to the lost (deposited) charge. The degree of saturation depends on both the intensity of light striking the PMT photocathode as well as the HV bias distributed across the dynode chain. The PMT output charge as a function of

* Work supported by the U.S. Department of Energy Office of Science, under contract number DE-AC02-06CH11357.

[†] jcdooling@anl.gov

the circulating current, I is modeled as [10],

$$Q_o(I) = \frac{AI}{(1 + BI^\alpha)^{1/\alpha}}, \quad (1)$$

where A , B , and α are determined from a specific fit. Data is fit using the sdds toolkit program `sddsgenericfit` [11]. Permitted values of α are constrained to the range of 0.25 to 4.0. Solving for I yields the deposited charge.

In ID01, where SCU1 is located, a single 61-FO cable bundle is located on the inboard side of the upstream (US) permanent magnet ID, and two 7-FO cable bundles are mounted within the cryostat. Calibration data for the ID01 fiber BLMs are presented in Figure 2 along with fits of the data to Eq. (1). The high voltage (HV) PMT bias is varied for the internal SCU1 inner and outer detectors, but kept at a fixed value of -600 V for the US monitor. The figures indicate that in-

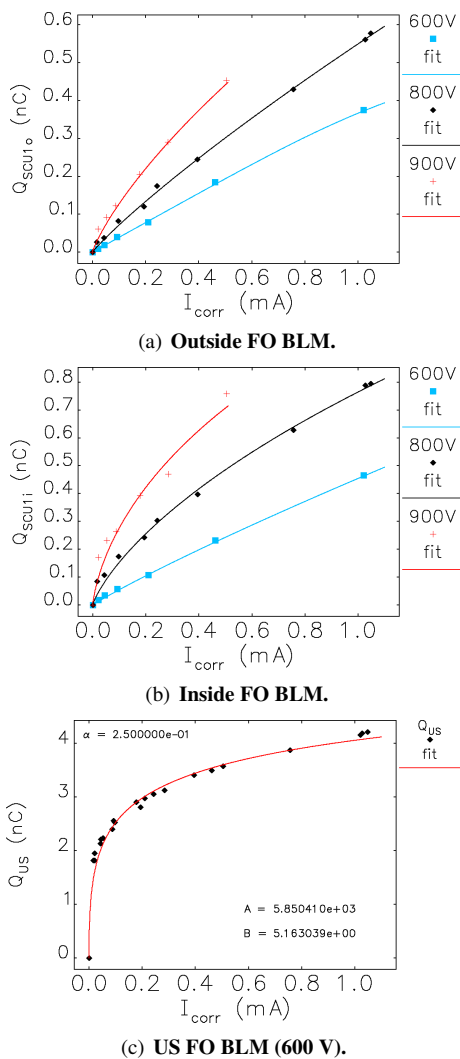


Figure 2: ID01 calibration data along with fits to Eq. (1).

creasing the bias pushes the PMT further into saturation at a given light level (assumed proportional to the corrected current, I_{corr}). Parameters for the fits are presented in Table 1. The gain $G(V)$ of the PMT goes approximately as

Table 1: Saturation Model Fit Parameters

Detector	Bias (V)	A (nC/mA)	B (mA $^{-\alpha}$)	α
SCU1i	-600 V	0.7073	0.1171	0.25
	-800 V	4.6707	0.5722	0.25
	-900 V	17.244	1.0332	0.25
SCU1o	-600 V	0.3886	0.2613	4.0
	-800 V	1.0185	0.1668	0.25
	-900 V	2.9575	0.4199	0.25
US	-600 V	5850	5.163	0.25

$G_o(V/V_o)^{N_d-1}$ where N_d is the number of dynodes; for these sub-miniature Hamamatsu R7400U-04 PMTs [12], $N_d = 8$. On the other hand, the available output charge is determined largely by the capacitance at the output end of the dynode chain; this varies linearly with HV bias. Therefore, a more linear response is expected at lower bias voltages. For large signals, however, reducing the PMT bias leads to oscillations in the output signals probably from the excessive space-charge generated at the photocathode that then has to be transported down the dynode chain. At higher bias voltages, increasing light signals cause the output pulse to temporally broaden.

ABORT KICKER BEAM LOSS

The APS SR abort kicker (AK) became operational at the end of the 2015 Run-1 user cycle [1, 13] for the purpose of preventing quenches of the SCU magnets due to beam dumps. The AK is triggered by the Machine Protection System (MPS) which relies principally on beam position limit detecting (BPLD) BPMs to determine when to dump the beam. Once triggered, the MPS mutes the rf drive signal to the cavity klystrons. Examples of fast BLM beam dump signals recorded in ID01 are presented in Figure 3, before and after the AK was operational. The PMT bias for both events was -800 V. In the first case, the SCU1 coils quenched;

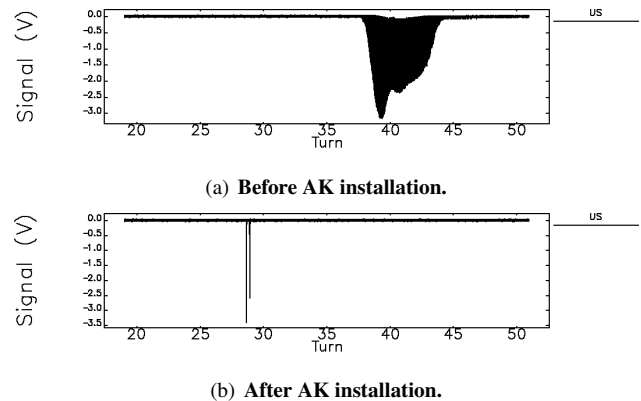


Figure 3: ID01 BLM signals before and after the AK became operational.

in the second case, they did not. The deposited charge in the case of no AK shown in Fig. 3(a) is 17.44 nC; with the AK (Fig. 3(b)) the charge drops to 56.7 pC. The losses in ID06 (SCU0) were much smaller for these two cases: 20.6 pC and below-detectable-limits for the respective events. The horizontal axes in Fig. 3 are given units of SR Turns (3.682 μ s/Turn). Turn=0 represents the moment when the MPS is triggered; this event is then used to trigger data collection oscilloscopes. After the beam loss data is saved, the scopes are automatically re-armed. The AK is timed to fire 90 μ s after the MPS trigger, equivalent to 24 Turns; therefore, FFOBLM signals are expected to appear after this time. Timing and settings for the AK are discussed in greater detail in Ref. [13].

The AK is not always as effective as the preceding example suggests. A second, independent protection mechanism known as the Personnel Safety System (PSS) switches off the SR dipole magnet power supply if conditions for possible radiation exposure are detected. In the case of a PSS trip, the MPS sometimes does not detect beam motion until a portion of the stored charge is already striking the vacuum chamber walls. In this case, the AK is not effective and the SC electromagnet coils can quench. An example of a PSS loss is given Figure 4. Here losses are present in ID06

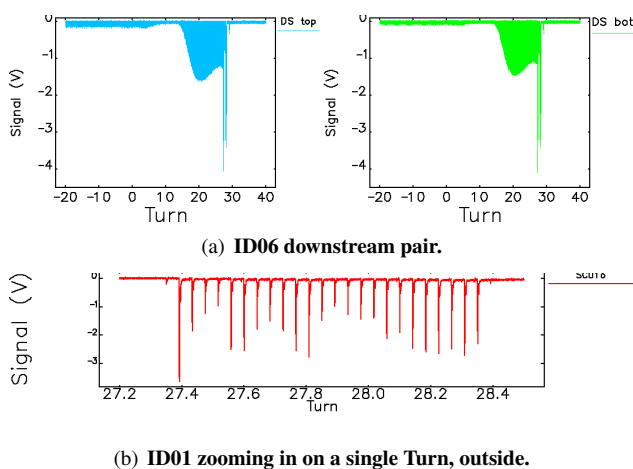


Figure 4: ID01 and ID06 early BLM signals from a PSS trip.

for ten's of Turns prior to the MPS trigger and AK firing; however, BLM signals in ID01 are not seen until after the AK trigger as shown in Fig. 4(b). The deposited charge levels in ID01 and ID06 were found to be 1.35 nC and 1.86 nC; both SCUs quenched. Because PSS-induced beam loss precedes that from the MPS we are working to have PSS trigger the MPS as well.

SUMMARY

As seen above, beam loss distributions are dynamic and can change from event to event. Because the distributions change, calibrations can only approximate the actual loss in SCUs. We find a rough beam loss threshold of 1 nC for

inducing SCU quenches. The threshold varies depending on loss power density and fluence as well as current in the SC magnet coils. Nevertheless, the fast BLMs have proven themselves as an invaluable diagnostic for examining loss dynamics, allowing us to properly adjust AK timing and amplitude. The FFOBLM must cover a broad dynamic range, detecting lost charge from sub-pC to nC; the saturation model given in Eq. (1) allows us to cover this range. Commercial systems are beginning to appear in the market [14]; however, we still seek to retain the fast time response and good spatial resolution the fibers provide. Sample rates of 1.25 GS/s and 2.5 GS/s are typically employed with the former being the most common; the slower of these two rates translates into a spatial resolution σ_t of roughly $\Delta t_s c/n = 0.2$ m. The FFOBLMs provide an important diagnostic with regard to timing. Early losses (before MPS triggering) had been observed previously [9]; however, their consequence was not fully appreciated until installation of the AK. The fast BLMs helped us to understand why the AK occasionally fails to prevent quenching of the SCUs during beam dumps; these events are associated with early losses.

ACKNOWLEDGMENTS

The authors wish to thank Louis Emery, Chuck Doose, Adam Brill, and Pat Dombrowski.

REFERENCES

- [1] K. Harkay *et al.*, "Development of an Abort Kicker at APS to Mitigate Beam Loss-induced Quenches of the Superconducting Undulator," in *Proceedings of IPAC2015*, Richmond, VA, USA, pp. 1787-1790.
- [2] T. Obina and Y. Yano, "Optical Fiber Based Loss Monitors for Electron Storage Rings," in *Proceedings of IBIC2013*, Oxford, UK, 638-643.
- [3] A. Kaukher *et al.*, "XFEL Beam Loss Monitor System," in *Proceedings of DIPAC2011*, Hamburg, Germany, 2011, 401-403.
- [4] A. Zhukov, "Beam Loss Monitors (BLMs): Physics, Simulations and Applications in Accelerators," in *Proceedings of BIW10*, Santa Fe, New Mexico, US, 2010, 553-565.
- [5] H. Henschel, M. Korfer, and K. Wittenburg, "Fiber Optic Radiation Sensing Systems for TESLA," TESLA Report No. 2000-26, September 2000, http://tesla.desy.de/new_pages/TDR_CD/PartII/chapter09/references/Tsakanov.pdf
- [6] F. Wulf *et al.*, "Beam loss Monitors for FEL using optical Fiber," *2009 IEEE Nuclear Science Symposium Conference Record*, N30-2, 1993-1997.
- [7] P. Gorodetzky *et al.*, *Nuclear Instruments and Methods in Physics Research A* 361 (1995) 161-179.
- [8] M. Wendt, "Challenges in Accelerator Beam Instrumentation," in *Proceedings of the DPF-2009 Conference*, Detroit, MI, USA, July 27-31, 2009, <http://arxiv.org/pdf/0912.1584.pdf>
- [9] J. Dooling *et al.*, "Calibration Of Fast Fiber-Optic Beam Loss Monitors For The Advanced Photon Source Storage Ring

- Superconducting Undulators," in *Proceedings of IPAC2015*, Richmond, VA, USA, pp. 1780-1782.
- [10] J. C. Dooling, K. C. Harkay, and Y. Ivanyushenkov, "Fast Beam Loss Diagnostic to Quantify Charge Deposition in APS Superconducting Undulators," *ICFA Beam Dynamics Newsletter*, 66, April 2015, p 24, <http://www-bd.fnal.gov/icfabd/Newsletter66.pdf>
- [11] http://www.aps.anl.gov/Accelerator_Systems_Division/Accelerator_Operations_Physics/manuals/SDDStoolkit/SDDStoolkitsu42.html
- [12] http://ctf3-tbts.web.cern.ch/ctf3-tbts/instr/PMT/R7400U_TPMH1204E07.pdf
- [13] K. Harkay *et al.*, "Operational experience with beam abort system for superconducting undulator quench mitigation," presented at the 2016 North American Particle Accelerator Conference (NAPAC16), Chicago, USA, Oct 2016, this conference.
- [14] K. B. Scheidt and P. Leban, "Prototype Results with a Complete Beam Loss Monitor System Optimized for Synchrotron Light Sources," in *Proceedings of IPAC2015*, Richmond, VA, USA, pp. 1019-1021.